RSC Advances

ROYAL SOCIETY OF CHEMISTRY

www.rsc.org/advances

Cite this: DOI: 10.1039/c0xx00000x

www.rsc.org/xxxxxx

ARTICLE TYPE

A reformative oxidation strategy using high concentration nitric acid for enhancing emission performance of graphene quantum dots

Taili Shao,[a,b] Guodong Wang,[b] Xuting An,[a] Shujuan Zhuo,[a] Yunsheng Xia,*[a] Changqing Zhu*[a]

Received (in XXX, XXX) Xth XXXXXXXXX 20XX, Accepted Xth XXXXXXXXX 20XX

DOI: 10.1039/b000000x

A highly concentration nitric acid oxidation strategy has been presented for one-step fabrication of strongly red-emitting fluorescent graphene quantum dots (GQDs) using activated carbon as carbon source. In optimal conditions, the emission quantum yield at 600 nm wavelength is as high as 18%. The concentration of the used nitric acid is critical to the optical properties of the GQDs: Concentrated nitric acid (14.6 M) can more sufficiently oxidize GQDs surface and more efficiently dope N element, resulting in longer emission band and higher emission efficiency. Preliminary cell image study indicates the obtained GQDs possess high signal to background ratio, good stability and low cytotoxicity, which endow their promising as a new type of near-infrared fluorophores for biological applications.

1. Introduction

Fluorescent carbon dots have attracted rising attention in biological applications owing to their more stable fluorescence and better biocompatibility, as compared with conventional semiconductor quantum dots and organic dyes.[1,2] In general, a desirable fluorescent cell label or biological image system should avoid endogenous auto-fluorescence background, decrease tissue damage and possess deep penetrability, which is often achieved by near-infrared (NIR) fluorophores.[3-5] Although the emission band of some carbon dots can be extended to NIR region based on their excitation-dependent emission behavior, the resultant emission intensity is too weak.[6-10] Tedious surface passivation or doping treatments are usually needed to improve the quantum yield (QY).[11-13] Thus, to effectively push the use in biological field, it is urgent to prepare high quality fluorescent carbon dots.

As a simple and convenient approach, nitric acid oxidation bears the merits of using facile oxidant and being applicable for different precursors.[14-20] Obviously, it would get more wide applications in various fields if the emission performances of carbon dots can be further enhanced. It should be noted that present oxidation method mostly employs relative low nitric acid concentration, which is not in favour of more sufficient surface oxidation and more efficient N element doping. Recently, Hu et al. indicate that the significant increase of oxygen segment can lead to the strong fluorescence.[21] Wepasnick and co-workers demonstrate that the level of oxidation is controlled by the oxidant concentration. Then the oxygen content in multi-walled carbon nanotubes can increase from 4.3 to 9.5% as the concentration of nitric acid enhances from 20 to 70% w/w.[22] Inspired by these studies, we propose whether we can choose higher concentrated nitric acid to enhance the oxidation degree and even obtain better N doping in carbon dots preparation.

In this study, we have presented a simpler but more effective strategy for the fabrication of bright red-emitting graphene quantum dots (GQD, one of carbon dots) based on nitric acid oxidation. Different from previous report,[14] we herein employ extremely concentrated nitric acid (14.6 M) as oxidant (instead of the mostly used 5 M nitric acid), for the preparation of the GQDs. To demonstrate the significance of nitric acid concentration, the commonly used activated carbon is chosen as carbon source. The present reformative oxidation strategy can not only obtain a well oxidation of GQDs surface but realize higher content of N element doping (4.31%). As a result, the obtained GQDs have 18% emission quantum yield at 600 nm wavelength, and no any additional surface modification and/or doping processes are needed. Furthermore, the obtained GQDs can be used for cell imaging, indicating that they are very promising as a new type of near-infrared fluorophores for biological applications.

2. Experimental section

2.1 Materials

Nitric acid (65-68%, ~14.6 M, analytically pure), activated carbon (Charcoal activated, powder, analytically pure, Item No. 10006619), dimethyl sulfoxide (DMSO) were obtained from Sinopharm Chemical Reagent Co, Ltd (Shanghai, China). Water used for the separation and purification of GQDs was from a water purification system (PSDK2-10-C). Fetal bovine serum (FBS), Kaighn's Modification of Ham's F-12 Medium (F12K Medium), Trypsinase Hanks balanced salt solution, Phosphate-buffered saline (PBS), 3-(4, 5-dimethylthiazol-2-yl)-2 and 5-diphenyl tetrazolium bromide (MTT) and CHO-K1 cells were purchased from Wuhan Boster Biological Engineering Co., Ltd (Wuhan, China).

2.2 Instruments and characterization

Fluorescence measurements were performed on F-4500 spectrofluorometer (Hitachi, Japan) equipped with a R3896 red-

sensitive multiplier and a 1 cm quartz cuvette upon excitation at 380-640 nm with a slit width of 10 nm. UV-Vis absorption spectrum was measured on a U-2910 spectrometer (Hitachi, Japan). Transmission electron microscopy (TEM) images were recorded by Tecnai G2 20 ST (FEI) under the accelerating voltage of 200 kV. Atom force microscopic (AFM) topography images were acquired from an Innova scanning probe microscope. Surface chemical bonding state was analysed by X-ray photoelectron spectroscopy (XPS, ESCALAB250, Thermo Scientific, USA). Fourier transform infrared (FT-IR) measurements were carried out with a FT-IR spectrometer using a KBr plate (FTIS-8400S, Shimadzu, Japan). The absolute quantum yields of the GQDs were probed by a fluorescence spectrometer (Edinburgh Photonics PLS920). Fluorescence microphotographs and Cell viability were taken on the Inverted fluorescence microscope (IX51, OLYMPUS, Japan) and Epoch microplate spectrophotometer (BioTek Instruments, Inc., USA), respectively.

2.3 Preparation of the GQDs

The GQDs were prepared by the oxidation of activated carbon in the presence of concentrated nitric acid. Typically, a mixture of 0.01 g of activated carbon and concentrated nitric acid (14.6 M, 20 mL) was refluxed using an oil bath maintaining a temperature of 140 degree centigrade for 3 h under violently stirring. The carbon particles with large size were eliminated from the resulted solution directly by centrifugation at 10000 rpm after the reaction cooled down to room temperature. GQDs with desired size were extracted by ethyl acetate and were further washed by water to remove excessive nitric acid. Finally, brown GQDs were harvested from the organic phase through the use of rotary evaporation system to remove the solvent. The synthesis route is depicted in Scheme 1.

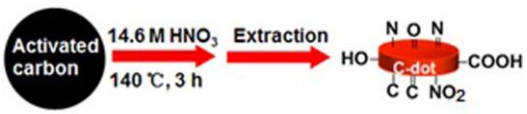

Scheme 1 Graphical representation of the synthesis route of the GQDs.

2.4 Quantum yield measurements

The absolute quantum yield (η) of as-prepared GQDs was measured by Edinburgh Photonics PLS920 fluorescence spectrometer according to the equation (1). Where ε and α represent photons emitted and absorbed by the sample, respectively. In the experimental procedures, the luminescence emission spectrum ($L_{emission}$), excitation spectrum after the exciting of specimen (E_{sample}) and the solvent ($E_{solvent}$) were measured by a calibrated integrating sphere.

$$\eta = \frac{\varepsilon}{\alpha} = \frac{\int L_{emission}}{\int E_{solvent} - \int E_{sample}} \quad (1)$$

2.5 Cell culture, inverted microscopy and cytotoxicity assay

CHO-K1 cells were cultured in 96-well plates with F12K medium containing 10% FBS at 37 ℃ in a 5% CO_2/95% air incubator for 24 h to obtain a suitable density (70-80% confluence). For bioimaging investigation, 10 μL of as-prepared GQDs suspension (0.5 mg mL^{-1}) was added into the test cell culture. The medium was removed and the cells were washed thoroughly twice by PBS after an incubation of 24 h. The washed cells were imaged under bright field, and green light excitation, respectively.

The cytotoxicity of the as-prepared GQDs was assessed by MTT method. Specifically, CHO-K1 cells cultured in 96-well plates incubated with different volume of GQDs (5.0, 10.0, 12.5, 15.0, 20 μL, 0.5 mg mL^{-1}). All cultures were incubated for 24 h at 37 ℃ in a 5% CO_2/95% air incubator. Then, 200 μL fresh medium of 20 μL MTT (5 mg mL^{-1} in PBS) was introduced into the well after the medium containing the GQDs was removed. The cells were incubated for another 4 h. Finally, all medium was removed and 200 μL DMSO was added, followed by shaking for 15 min. The absorbance of each well was measured at 490 nm using Epoch microplate spectrophotometer with pure DMSO as a blank. Non-treated cells (in F12K) were used as a control and the relative cell viability (mean% ± SD, n = 3) was expressed as $Abs_{sample}/Abs_{control} \times 100\%$.

3. Results and discussion

The size distribution of the as-prepared GQDs was evaluated by TEM as shown in Fig. 1A, indicating that the size of them located in a short range from 3.3 to 12 nm with an average diameter of 7 nm. The high resolution TEM (HRTEM) image (inset in Fig. 1A) displays a lattice spacing distance of 0.22 nm, which is similar to that of (100) facet of graphite carbon. Their height is only 2-3 nm based on AFM measurement (Fig. 1B). So, the as-prepared GQDs are flat (Scheme 1) rather than pseudo-spherical.

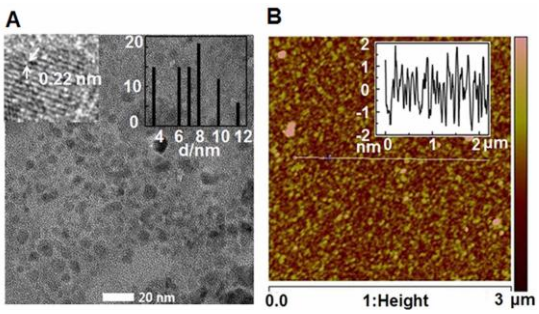

Fig. 1 (A) TEM, HRTEM (left insert) images, and size distribution (right insert) of the as-prepared GQDs. (B) The AFM image of the as-prepared GQDs with the height profile along the line in the image.

The absorption and fluorescence spectra of as-prepared GQDs were then investigated. As presented in Fig. 2A, several obvious absorption shoulders ranging from 350 to 400 nm and a typical absorption edge extending to the visible range were observed from the UV-Vis absorption spectrum of GQDs. These absorption features indicated that the GQDs possessed many chromophores (such as O-C=O, C=N, C=C, N=O). As excitation wavelength increased from 380 to 640 nm, the emission from the GQDs gradually shifted to longer wavelengths (Fig. 2B). This excitation-dependent fluorescence behavior is one of most special properties of GQDs. The maximum emission peak was at 600 nm as the GQDs were excited at 520 nm. As far as we know, the emission located at 600 nm upon excitation at 520 nm is the longest wavelength of the maximum emission for the GQDs reported (Table S1). The absolute quantum yields at 600 and at

636 nm are 18% and 6%, respectively, measured by calibrated integrating sphere. Such highly emitting property is very rare for near-infrared GQDs.

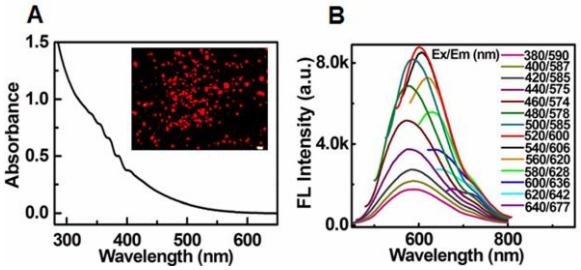

Fig. 2 (A) UV-Vis absorption spectrum of the as-prepared GQDs dispersed in ethyl acetate solution. Insert: the inverted fluorescence microphotograph of the GQDs on the glass slide under green light excitation. (B) The fluorescence spectra of the as-prepared GQDs in ethyl acetate solution at different excitation wavelengths.

It is interesting to ask why the as-prepared GQDs possess so favourable optical properties. To try to answer this question, their composition and chemical binding states were studied. The FT-IR spectrum (Fig. 3A) exhibits distinct absorption bands at 3419, 1724, 1600, 1535 and 1345, 1250, 1100, 870 cm^{-1}, corresponding to the groups of NH/OH (HO-C=O), C=O, C=C, N=O, C-N, C-O, C-N (C-NO_2), respectively. These results well agreed with UV-Vis absorption data. For a better understanding, Element analysis and XPS measurements were performed. The GQDs contain C, O, N, H four elements, and their contents are 57.13, 32.12, 4.31 and 4.10%, respectively. The doping N is as high as 4.31%, which is the highest content among the GQDs made by nitric acid oxidation (Table S2).

The N1s spectrum (Fig. 3B) displays three peaks at 399.9, 401.1 and 406.5 eV, which are attributed to C-N, C=N and N=O, which indicate that the N is mainly bonding to carbon. It was reported that only N bonding to carbon in GQDs could enhance the emission by inducing an upward shift of the Fermi level and electrons in the conduction band.[23,24] For GQDs, the N bonding to carbon disorders the carbon hexagonal rings and creates emission energy traps for the particles through the radiative recombination induced by electron-hole pairs, which lead to a higher QY.[25,26] Simultaneously, the emission peaks of the GQDs with increasing N contents would shift to a longer wavelength under the same excitation wavelength according to Zhang's report.[27] So the form of N-C bond and high N contents might be responsible for the high QY and long wavelength emission of the as-prepared GQDs.

The spectrum of C1s (Fig. 3C) shows five peaks at 284.4, 285.0, 285.6, 286.2, 289.5 eV, corresponding to C=C (sp^2), C-C (sp^3), C-O/C-N, C=N/C=O and O-C=O, respectively. The appearance of a peak at the binding energy of 284.4 eV indicates the presence of graphitic sp^2 carbon structure.[18] As well-known, activated carbon is an amorphous form of carbon, which contains abundant graphite components, mostly likely tiny fragments of crystalline graphite. So, activated carbon is a more ideal carbon source than pure graphite for fabrication of GQDs. Based on previous study, GQDs with predominantly sp^2 graphitized crystalline carbon core is particle size-dependent.[28] Larger GQDs showed longer emission wavelength due to quantum-confinement effects. That is, the maximum peak wavelength was dependent on the average sizes of the GQDs. Average diameter of 7 nm of as-prepared GQDs is much larger than those prepared by other methods (Table S2), which play a pivotal role for their near-infrared emission.

The O1s spectrum (Fig. 3D) consists of three peaks at 532.1, 532.6, 533.8 eV, which are ascribed to C-O, C=O/N=O and C=O. It is well-known that nitric acid oxidation can incorporate N and O into the GQDs and produce OH and COOH groups on the GQDs surfaces.[17] Simultaneously, the fluorescence quantum yield of GQDs depends on the efficiency of N and O incorporation. Moreover, the oxidation level was controlled by the oxidant concentration.[22] That is, the greater the concentration, the higher content the oxygen. Higher oxidation degree, more N doping and larger sizes have been realized simultaneously using concentrated nitric acid (14.6 M) as oxidation, which might be the most important reason for high QY and near-infrared emission.

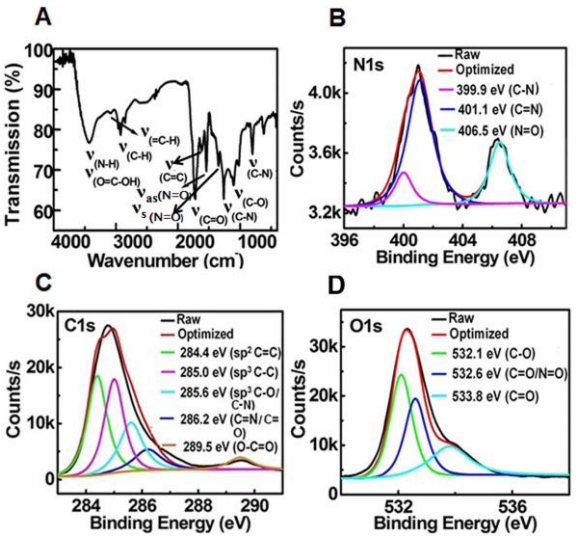

Fig. 3 (A) FTIR and XPS spectra of (B) N1s, (C) C1s, (D) O1s of the as-prepared GQDs.

Based on above results, we considered that the concentration of the used nitric acid was critical. To verify this speculation, the control experiments for studying the effect of nitric acid concentration were conducted. We fabricated GQDs by using 8 M nitric acid, and then studied their sizes, compositions and fluorescence properties. As showed in Fig. 4, the size distribution ranges from 2.6-6 nm, and average diameter is 3.7 nm, which is much smaller than GQDs oxidized by concentrated nitric acid. Furthermore, their N atom content was only 1.1%, which was much lower than that of the highly emitting GQDs (4.31%). The unusual results caused our attention. It is well-known that nitric acid oxidation introduces functional groups (such as OH, COOH, NO_2, etc.) on the carbon particles surfaces, which made them hydrophilic and negatively charged particles.[29] Simultaneously, this oxidation can also induce a small extent of nitration into carbon particles.[30,31] In addition, it helps to break the large aggregated activated carbon particle into small GQDs. Concentrated nitric acid oxidation could produce more abundant surface oxygen functional groups and larger N content than diluted nitric acid, and might delay the break process and cause the larger particles size. Obviously, the detailed mechanism should be further studied.

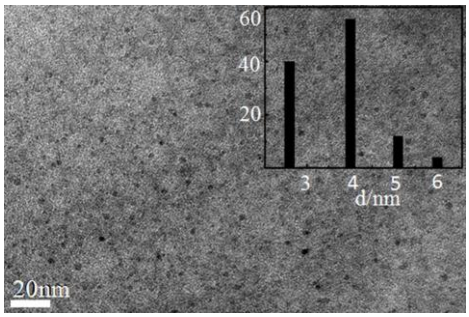

Fig. 4 The TEM image of the GQDs synthesized by 8 M nitric acid. Insert: the size distribution.

As expected, the emission bands of GQDs obtained from 8 M diluted nitric acid exhibited an obvious hypsochromic shift under the same excitation (Fig. S1C), and the maximum emission was blue-shifted to 541 nm with a lower quantum yield of 5%. To further investigate the effects of nitric acid concentration on the properties of GQDs, two moderate concentrations of nitric acid (12 and 10 M) were also used to synthesize GQDs. As can be seen from Fig.S1, the maximum emission wavelengths were 587 nm (Fig. S1A) with QY of 8.7% for 12 M nitric acid and 563 nm (Fig. S1B) with QY of 6.1% for 10 M nitric acid, respectively. The fluorescence wavelengths and QYs obtained from different concentrations of nitric acid were summarized in Table S3. These results clearly indicate that the concentration of nitric acid has profoundly effects on the optical properties of the products, namely, the higher concentration of the used nitric acid, the longer emission wavelengths and higher QYs of the obtained GQDs.

To further demonstrate the excellent and universal preparation method of GQDs, concentrated nitric acid oxidation treatment of another carbon source was performed. When alcohol lamp soot was used as carbon source, more N content (7.06%) and higher QY (50%) were obtained. Our assumption was further confirmed by above results that high QY ascribed to the high N contents and sufficient oxidation by concentrated nitric acid. The maximum emission peak is at 538 nm with excitation of 480 nm (Fig. S2), and average diameter is 2.8 nm judged from TEM image (Fig. S3), indicating that fluorescence of the obtained GQDs from alcohol lamp soot is also particle size-dependent, which is consistent with the usual fluorescence behavior of sp^2 crystalline GQDs. Here, the differences of GQDs sizes might be attributed to the differences of carbon source.

Due to bright red fluorescence, the as-prepared GQDs were promising for bio-labeling and bio-imaging. To evaluate their practicability, CHO-K1 cells were chosen as a model system and imaging experiments were conducted by an inverted fluorescence microscope. As shown in Fig. 5A, the CHO-K1 cells incubated with the GQDs became bright red under green light excitation, demonstrating that the GQDs were successfully internalized by CHO-K1 cells. Moreover, GQDs are quite stable in cells as fluorescence intensity of the labeled cells exhibited no obvious reduction even after 48 h incubation (Fig. 5C). No fluorescent was observed from CHO-K1 cells in the absence of GQDs in the control sample (Fig. 5E), implying that the GQDs could be used as cell imaging agent with a high signal to background ratio. This point is further supported the low cytotoxicity of as-prepared GQDs. The cell activity didn't showed obvious change when 20 μL of GQDs (0.5 mg mL^{-1}) to add into culture medium as tested by the MTT assay (Fig. S4).

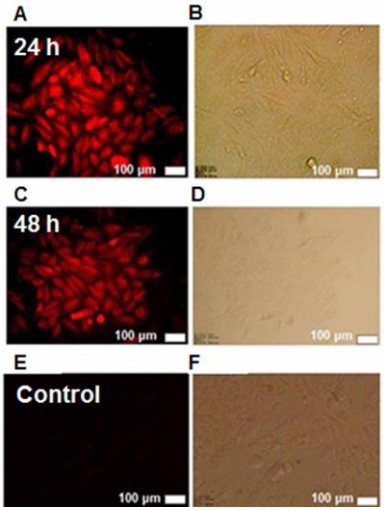

Fig. 5 Cellular imaging of CHO-K1 cells using the as-prepared GQDs. A-D: Fluorescence under green light excitation and bright field cell image after different incubation time GQDs (A, B 12 h and C, D 48 h). E and F: Control cells experiments without addition of GQDs. The scale bar is 100 μm.

4. Conclusions

Red highly-emitting GQDs were fabricated by simple and one-step concentrated nitric acid oxidation strategy. They not only act as a novel candidate of near-infrared fluorophores, but well enrich the properties and applications of carbon-based nanomaterials. In addition, the GQDs have several advantages. First, they are amphiprotic. The as-prepared GQDs can well dissolve in a series of mediums (such as N, N-dimethylformamide, water, alcohol, ethyl acetate) and form transparent solutions (Fig. S5). Such versatile solubleness facilitates to extend their applications. Then, the fabrication is very low-cost and time-saving. Both activated carbon and nitric acid are commercially obtained. Furthermore, the GQDs can be reliably obtained by one simply oxidation step within 3 h, any tedious polymer coating or post-treatments are needless. Third, the surface possesses many OH, COOH groups, which can be used for further conjunction reactions.

This work was supported by the National Natural Science Foundation of China (Nos. 21375003, 21175003, C.Z.; 21303003, S.Z).

Notes and references

[a] *Anhui Key Laboratory of Chemo-Biosensing, College of Chemistry and Materials Science, Anhui Normal University, Wuhu 241000, People's Republic of China. Tel: +86 553 3937137, Fax: +86 553 3869303; E-mail: xiayuns@mail.ahnu.edu.cn; zhucq@mail.ahnu.edu.cn*

[b] *School of Pharmacy, Wannan Medical College, Wuhu 241002, People's Republic of China.*

† Electronic Supplementary Information (ESI) available: Experimental details of figures concerning fluorescence, TEM, Cell viability assay, a summary of fluorescence characterization and a comparison of morphology and composition.. See DOI: 10.1039/b000000x

1 S. N. Baker, G. A. Baker, *Angew. Chem. Int. Ed*., 2010, 49, 6726.

2 H. T. Li, Z. H. Kang, Y. Liu, S. T. Lee, *J. Mater. Chem*., 2012, 22, 24230.

3 D. H. Tian, Z. S. Qian, Y. S. Xia, C. Q. Zhu, *Langmuir*, 2012, **28**, 3945.

4 H. Y. Ko, Y. W. Chang, G. Paramasivam, M. S. Jeong, S. Cho, S. Kim, *Chem. Commun*., 2013, **49**, 10290.

5 M. Nurunnabi, Z. Khatun, G. R. Reeck, D. Y. Lee, Y. K. Lee, *Chem. Commun.*, 2013, **49**, 5079.

6 R. L. Liu, D. Q. Wu, S. H. Liu, K. Koynov, W. Knoll, Q. Li, *Angew. Chem. Int. Ed*., 2009, **48**, 4598.

7 H. T. Li, X. D. He, Z. H. Kang, H. Huang, Y. Liu, J. L. Liu, S. Y. Lian, C. H. A. Tsang, X. B. Yang, S. T. Lee, *Angew. Chem. Int. Ed*., 2010, **49**, 4430.

8 L. Bao, Z. L. Zhang, Z. Q. Tian, L. Zhang, C. Liu, Y. Lin, B. P. Qi, D. W. Pang, *Adv. Mater*., 2011, **23**, 5801.

9 Y. Xu, M. Wu, X. Z. Feng, X. B.Yin, X. W. He, Y. K. Zhang, *Chem. Eur. J*., 2013, **19**, 6282.

10 X. Y. Li, H. Q. Wang, Y. Shimizu, A. Pyatenko, K. Kawaguchi, N. Koshizaki, *Chem. Commun*., 2011, **47**, 932.

11 H. Peng, J. Travas-Sejdic, *Chem. Mater*., 2009, **21**, 5563.

12 Y. Q. Dong, H. C. Pang, H. B.Yang, C. X. Guo, J. W. Shao, Y. W. Chi, C. M. Li, T. Yu, *Angew. Chem. Int. Ed*., 2013, **52**, 7800.

13 L. Cao, X. Wang, M. J. Meziani, F. Lu, H. Wang, P. Luo, Y. Lin, B. A. Harruff, L. M. Veca, D. Murray, S.-Y. Xie, Y. P. Sun, *J. Am. Chem. Soc*., 2007, **129**, 11318.

14 Z. A. Qiao, Y. F. Wang, Y. Gao, H. W. Li, T. Y. Dai, Y. L. Liu, Q. S. Huo, *Chem. Commun*., 2010, **46**, 8812.

15 Y. Liu, C. Y. Liu, Z. Y. Zhang, *J. Colloid Interface Sci*., 2011, **356**, 416.

16 X. Y. Xu, R. Ray, Y. L. Gu, H. J. Ploehn, L. Gearheart, K. Raker, W. A. Scrivens, *J. Am. Chem. Soc*., 2004, **126**, 12736.

17 S. C. Ray, A. Saha, N. R. Jana, R. Sarkar, *J. Phys. Chem. C*, 2009, **113**, 18546.

18 Y. Q Dong, N. N. Zhou, X. M. Lin, J. P. Lin,Y. W. Chi, G. N. Chen, *Chem. Mate*r. 2010, 22, 5895.

19 K. M.Tripathi, A. K. Sonker, S. K. Sonkar, S. Sarkar, *RSC Adv*., 2014, **4**, 30100.

20 R. Ye, C. S. Xiang, J. Lin, Z. W. Peng, K. W. Huang, Z. Yan, N. P. Cook, E. L. G. Samuel, C. Hwang, G. D. Ruan, G. Ceriotti, A. O. Raji, A. A. Martí, J. M. Tour, *Nature Communicatio*ns, DOI: 10.1038/ncomms3943.

21 L. M. Hu, Y. Sun, S. L. Li, X. L. Wang, K. L. Hu, L. R. Wang, X. J. Liang, Y. Wu, *Carbon*, 2014, **67**, 508.

22 K. A. Wepasnick, B. A. Smith, K. E. Schrote, H. K. Wilson, S. R. Diegelmann, *Carbon*, 2011, **49**, 24.

23 Y. Xu, M. Wu, Y. Liu, X. Z. Feng, X. B. Yin, X. W. He, Y. K. Zhang, *Chem. Eur. J*., 2013, **19**, 2276.

24 P. Ayala, R. Arenal, A. Loiseau, A. Rubio, T. Pichler, *Rev. Mod. Phys*. 2010, **82**, 1843.

25 A. B. Bourlinos, A. Stassinopoulos, D. Anglos, R. Zboril, M. Karakassides, E. P. Giannelis. *Small*, 2008, **4**, 455.

26 S. Liu, J. Q. Tian, L. Wang, Y. L. Luo, J. F. Zhai, X. P. Sun, *J. Mater. Chem*., 2011, **21**, 11726.

27 Y. Q. Zhang, D. K. Ma, Y. Zhuang, X. Zhang, W. Chen, L. L. Hong, Q. X. Yan, K. Yu, S. M. Huang, *J. Mater. Chem*. 2012, **22**, 16714.

28 B. C. Zhu, S. Y. Sun, Y. F. Wang, S. Deng, G. N. Qian, M. Wang, A. G. Hu, *J. Mater. Chem. C*, 2013, **20**, 580.

29 H. P. Boehm, *Carbon*, 1994, **32**, 759.

30 I. I. Salame, T. J. Bandosz, *J. Colloid Interface Sci*., 2001, **240**, 252.

31 K. Kamegawa, K. Nishikubo, M. Kodama, Y. Adachi, H. Yoshida, *Carbon*, 2002, **40**, 1447.